The following supplement accompanies the article

Active hunting by deep-diving sperm whales: 3D dive profiles and maneuvers during bursts of speed

Kagari Aoki[1,*], Masao Amano[2], Kyoichi Mori[3,6], Aya Kourogi[2], Tsunemi Kubodera[4], Nobuyuki Miyazaki[5]

[1]International Coastal Research Centre, Atmosphere and Ocean Research Institute, The University of Tokyo, Otsuchi, Iwate 028-1102, Japan
[2]Faculty of Fisheries, Nagasaki University, Bunkyo, Nagasaki, 852-8521, Japan
[3]Ogasawara Whale Watching Association, Chichijima, Ogasawara, Tokyo 100-2101, Japan
[4]Department of Zoology, National Science Museum, Tokyo, Shinjuku, Tokyo 169-0073, Japan
[5]Center for International Cooperation, Ocean Research Institute, The University of Tokyo, Nakano, Tokyo 164-8639, Japan
[6]*Present address:* Department of Animal Sciences, Teikyo University of Science & Technology, Uenohara, Yamanashi 409-0193, Japan

*Email: aokikagari@aori.u-tokyo.ac.jp

Marine Ecology Progress Series 444:289–301 (2012)

Supplement: Tag design and data analysis

Suction-cup attached tags

We used 2 different types of suction-cup attached tags, with designs based on the type of data logger used. Each tag included a data logger, a suction cup (Canadian Tire), a float made of synthetic foam, and a VHF radio transmitter (Advanced Telemetry Systems). The PDT data logger with a vertical tail fin was attached to a suction cup with a rotating plate (see Aoki et al. 2007a,b for details; Fig. S1) and referred to as Type A (the float—length: 16 cm, width: 9 cm, thickness: 2 cm; see Fig. S1 for the detailed design). This tag was modified from a tag used in several previous studies (e.g. Hooker & Baird 1999, see Aoki et al. 2007a,b for detailed modification of the tag). The design of Type A tags ensures that the data loggers align with the water stream (Aoki et al. 2007a,b). The weight of the entire tag was 470 g. The design of tags using PD2GT and 3MPD3GT data loggers (Type B tags) differed from that of Type A tags and were the modified versions of those used in a study by Akamatsu et al. (2005) (Fig. S1). The length, width, and thickness of the float for the Type B tag were 21, 4, and 5 cm, respectively (see Fig. S1 for the detailed design). The weight of the entire tag was from 370 to 410 g. For Type B tags, the data loggers were fixed on suction cups; this enabled the measurement of acceleration and magnetic field changes caused by the whales' movements. However, because the data loggers were fixed, there were concerns that swim speed would not be accurately measured if the data logger did not always align with the water stream.

We attached both Type A and B tags to one of the whales to compare the swim speeds measured by each type. The data for swim speed were similar for both types of tags. We obtained a linear regression line of swim speed measured by the Type B tag against swim speed measured by the Type A tag. Although the coefficient of the slope was slightly <1 (0.96), the regression coefficient was relatively high (0.93). We therefore concluded that data loggers in Type B tags aligned with the water stream and assumed that the heading of the data logger did not differ dramatically from that of the tagged whales. Sakai et al. (2011) showed that Type B tags were not initially deployed parallel to the body axes of animals (Fig. 2a,c,e in Sakai et al. 2011), but they shifted to an almost parallel position after several minutes and remained in that position for at least 3 h (Fig. 2b,d,f in

Sakai et al. 2011). However, we were unable to check the tag position at every surfacing for all the tagged whales. The heading of the data-loggers therefore may not be exactly parallel to the body axes of the whales. This might have caused estimates of speed to be under- or overestimated to some extent. Indeed, swim speed was slightly higher in this case. However, this should not have greatly affected the overall results.

Data analysis

Bursts of speed: To determine the whales' maneuvers, we investigated how many categories (i.e. pitch, roll, and heading) showed simultaneous (within ±3 s) rapid changes in body orientation and assigned to these changes a number between 0 and 3. For example, when rapid changes in body orientation were observed in any 2 categories of pitch, roll, and/or heading within ±3 s of each other, the categorical number was 2. Bursts were classified according to changes in depths (i.e. descent, horizontal movement, and ascent). Descent and ascent were specified as an increase or decrease in depth, respectively, of at least 20 m (about twice the body length). A combination of the 3 categories (i.e. descent, horizontal movement, and ascent) was also identified during a burst. We calculated the linearity during a burst as the straight-line distance divided by the total horizontal distance at 5 to 10 s intervals. Tagged whales were determined to be turning when linearity was <0.64 (linearity of a half circle: 0.64).

Twenty of the 181 bursts had periods when the rotation value of the data logger's propeller was zero, even though changes in depth were observed during the same period. Because 13 of the 20 of these occurred on 1 whale (ID O6b), we suggest that these values were caused by tag position. Another potential explanation for these cases was that whales might be drifting. The maximum speed, total distance, and ratio of locomotion cost of bursts to a whole dive were not calculated.

Generalized linear mixed models (GLMMs) were used in the R 2.6.2 package (The R Foundation for Statistical Computing, Vienna). The changes in deviance in GLMM analyses were used to determine significance for each variable. Changes in deviance approximated a chi-squared distribution when a variable was dropped from the full model with all explanatory variables. A GLMM analysis with a gamma error distribution and inverse link function was used to compare deceleration rates during bursts with those recorded during gliding. This statistical model included decelerating rates as a dependent factor, mean speed of decelerating periods and phase (glide/burst) as fixed independent factors, and whale ID as a random factor. In another case, a GLMM analysis with a Gaussian error distribution and identity link function was used. We investigated changes in pitch and heading during the deceleration period of the bursts. The model included decelerating rates as a dependent factor, average rates of change in pitch and heading and maximum swim speed during deceleration periods as fixed independent factors, and whale ID as a random factor.

Locomotion cost: Locomotion cost (M_L) was approximated based on estimates of hydrodynamic drag (Hind & Gurney 1997).

$$M_L = \frac{\lambda}{\varepsilon_A \varepsilon_P} \frac{\rho S C_D U^3}{2}$$

where ε_A is metabolic efficiency (0.25; Kleiber 1975); ε_P is propeller efficiency (0.75; Fish 2000); λ is the active-to-passive drag ratio (3; Weihs 1974); ρ is the density of seawater (kg m^3); S is the total surface area of the whale (m^2); C_D is the drag coefficient based on total surface area of the tagged whale (0.00306; Miller et al. 2004); and U is swim speed (m s^{-1}). Assuming that the tagged whale had a body length of 8 m (median of estimated body length), the body weight was estimated to be 7305 kg (Lockyer 1976), and the total surface area was estimated to be 23.7 m^2 (Miller et al. 2004). The density of seawater was calculated from the International Equation of State of Seawater (UNESCO 1981) by using depth (m) and water temperature (°C) recorded from data loggers and salinity (34.84‰; Vogel 1981).

LITERATURE CITED

Akamatsu T, Matsuda A, Suzuki S, Wang D and others (2005) New stereo acoustic data logger for free-ranging dolphins and porpoises. Mar Tech Soc J 39:3–9

Aoki K, Amano M, Yoshioka M, Mori K, Tokuda D, Miyazaki N (2007a) Diel diving behaviour of sperm whales off Japan. Mar Ecol Prog Ser 349:277–287

Aoki K, Amano M, Sugiyama N, Muramoto H and others (2007b) Measurement of swim speed in sperm whales. In: Proceedings of the international symposium on underwater technology 2007 and international workshop on scientific use of submarine cables and related technologies (UT07_SSC07). IEEE, Tokyo, p 467–471

Fish FE (2000) Biomechanics and energetics in aquatic and semiaquatic mammals: platypus to whale. Physiol Biochem Zool 73:683–698

Hind AT, Gurney WSC (1997) The metabolic cost of swimming in marine homeotherms. J Exp Biol 200:531–542

Hooker SK, Baird RW (1999) Deep-diving behaviour of the northern bottlenose whale, *Hyperoodon ampullatus* (Cetacea: Ziphiidae). Proc Biol Sci 266:671–676

Kleiber M (1975) The fire of life: an introduction to animal energetics. Huntington, Robert E. Krieger Publishing Company, New York, NY

Lockyer C (1976) Body weights of some species of large whales. ICES J Mar Sci 36:259–273

Miller PJO, Johnson MP, Tyack PL, Terray EA (2004) Swimming gaits, passive drag, and buoyancy of diving sperm whales (*Physeter macrocephalus)*. J Exp Biol 207:1953–1967

Sakai M, Aoki K, Sato K, Amano M and others (2011) Swim speed and acceleration measurements of short-finned pilot whales (*Globicephala macrorhynchus*) in Hawai‘i. Mamm Study 36:55–59

UNESCO (1981) Tenth report of the joint panel on oceanographic tables and standards. UNESCO Technical Papers in Marine Science, No. 36. UNESCO, Paris

Vogel S (1981) Life in moving fluids. The physical biology of flow. Willard Grant Press, Boston, MA

Weihs D (1974) Energetic advantages of burst swimming of fish. J Theor Biol 48:215–229

Table S1. Results of principal components analysis obtained by using parameters of bursts on 5 sperm whales tagged with the 3MPD3GT.

	Principal components		
	1	2	3
Eigenvalues	2.31	0.77	0.5
Percent of variance account for loadings:	57.8	19.3	12.6
Maximum speed	0.704	–0.621	0.007
Maximum deceleration	0.827	–0.178	0.233
Maximum rate of heading change	0.780	0.247	–0.574
Rapid and simultaneous changes in body orientation occurring in 1, 2, or all categories (pitch, roll, and heading)[a]	0.722	0.543	0.345

[a]See ‘Bursts of speed’ in the supplement

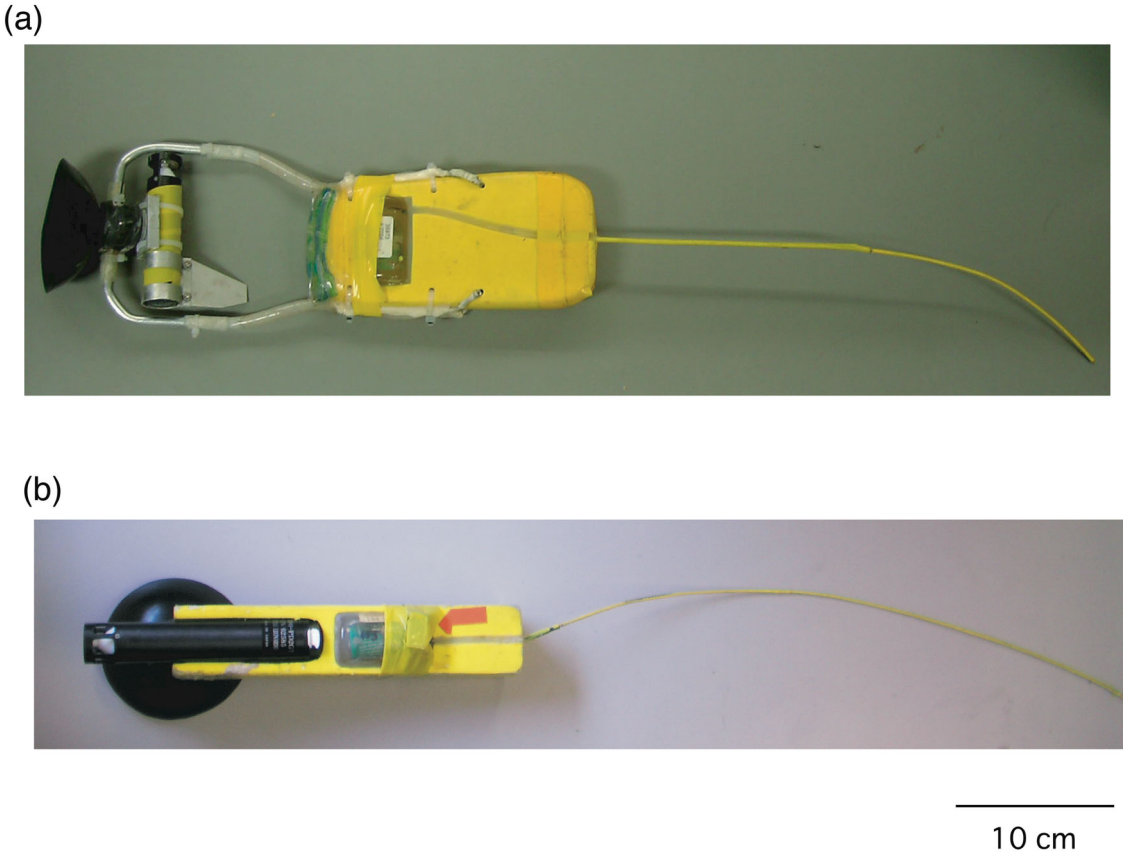

Fig. S1. Suction-cup attached tags. (a) Type A for the PDT data logger. (b) Type B for the PD2GT and the 3MPD3GT data loggers (see also Aoki et al. 2007a,b for the Type A tag)

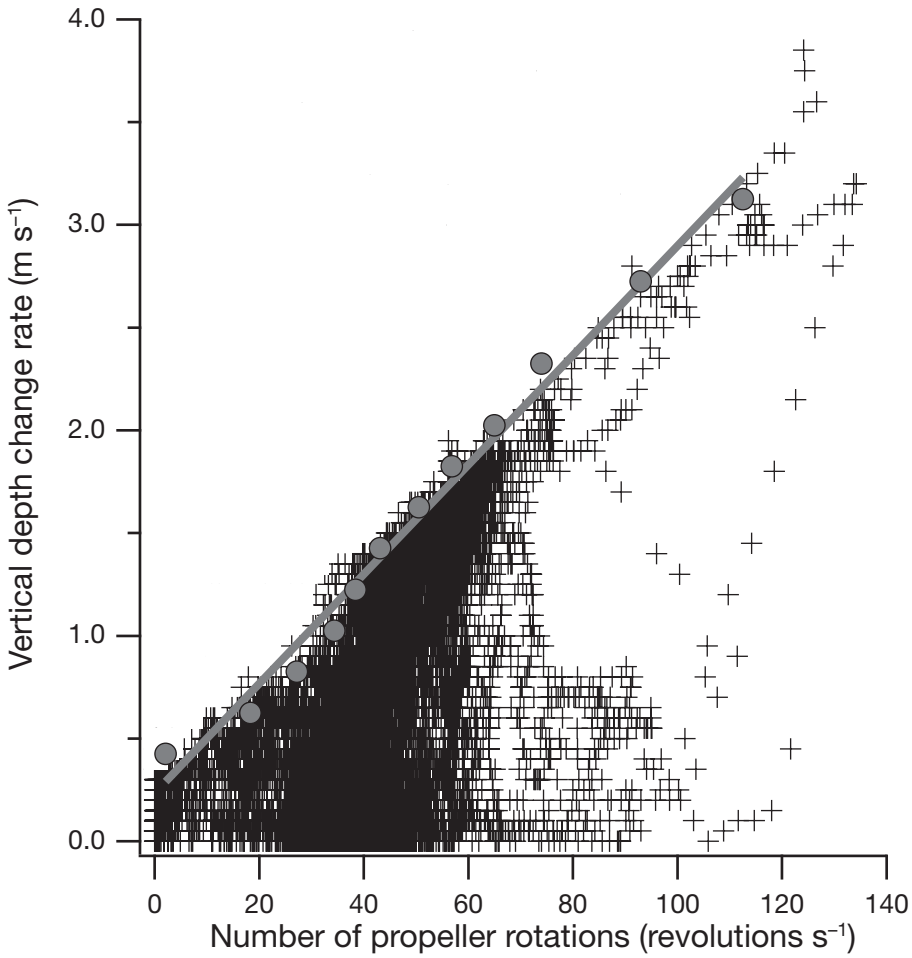

Fig. S2. An example of a calibration line calculated as the vertical depth change rate in relation to the number of propeller rotations for Whale O6c. We applied this method, as both PDT and PD2GT data loggers were used (see 'Materials and methods' for calibration methods). Mean propeller rotation values and vertical depth change rates were calculated at 10 s intervals. Because longer intervals give a high resolution of depth change rate, we used a longer interval than in the case illustrated in Fig. S3. We regressed third percentile points of propeller rotation data to corresponding vertical depth change rates for each whale's data (grey circles; see also Aoki et al. 2007a for details)

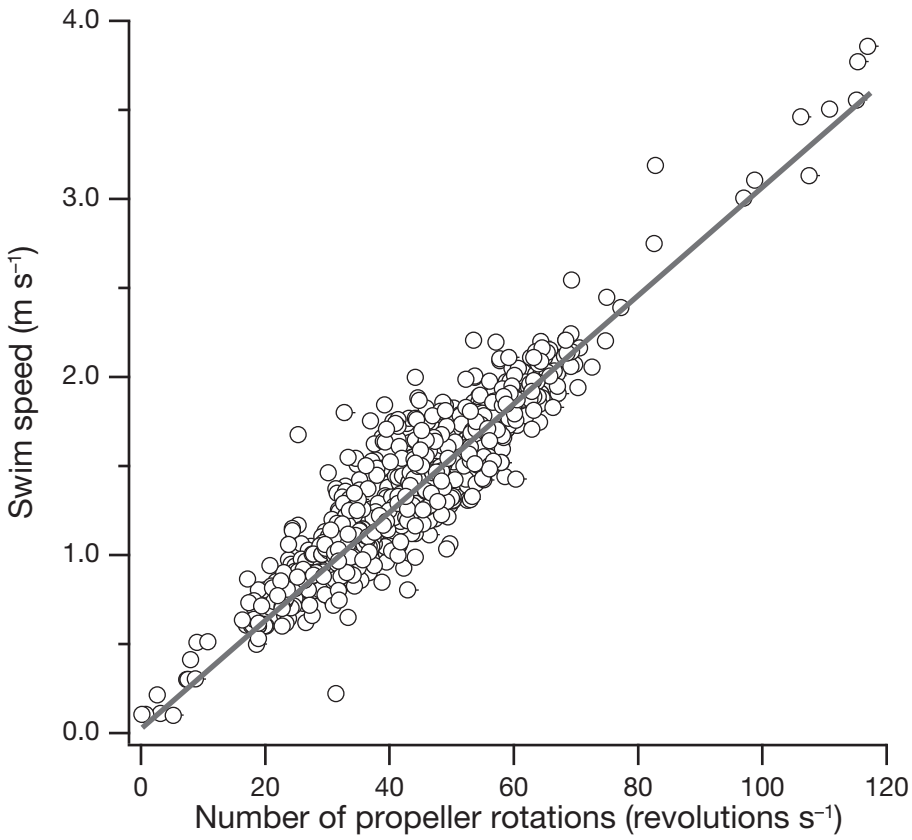

Fig. S3. An example of a calibration line calculated as the swim speed in relation to the number of propeller rotations for Whale O8k. Swim speed was calculated as the average depth change rate divided by the average sine of pitch at 5 s intervals when a steeper pitch was observed (i.e. $\sin \theta| >$ 0.9). The number of propeller rotations was also averaged at 5 s intervals. This method was applied for whales tagged with the 3MPD3GT data logger

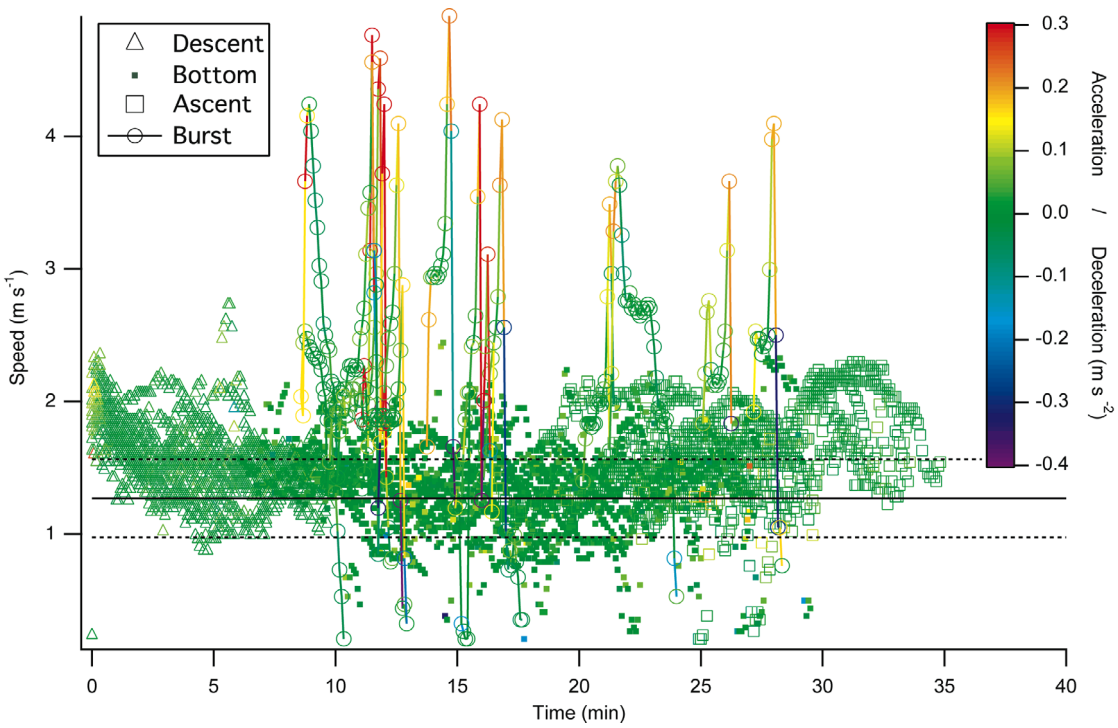

Fig. S4. Swim speed versus time for all data of Whale O8e. Time 0 marks the beginning of each dive. The black line shows mean swim speed during bottom phases. Dashed lines show the standard deviation. Colors indicate forward accelerations and decelerations. Bursts were expressed as events including relatively high speed with strong forward accelerations (forward acceleration > 0.15 m s^{-2} and swim speed > mean + 1.5 SD of the bottom phase of each dive). Higher speed without strong forward acceleration was not defined as a burst. Bursts occurred mostly in the bottom phases